Journal of Applied Research and Technology

www.jart.ccadet.unam.mx
Journal of Applied Research and Technology 16 (2018) 103-114

Original

An algorithm for wavelet thresholding based image denoising by representing images in hexagonal lattice

Jeevan K. M.*, S. Krishnakumar

School of Technology and Applied Sciences, Cochin, Kerala India.

Received dd mm aaaa; accepted dd mm aaaa
Available online dd mm aaaa

Abstract: The existing method of representation for digital images is using square shaped picture elements called pixels in a rectangular grid. Processing based on hexagonal grid is a new approach in image processing. It has various advantages like symmetry, higher angular resolution, consistent connectivity and higher sampling efficiency. Image processing applications like rotation, scaling, edge detection, and compression in hexagonal domain have already been discussed by many researchers. In this paper we propose an image denoising scheme in hexagonal lattice using wavelet thresholding method. For the thresholding of wavelet coefficients, modified NeighShrink thresholding method is applied. In NeighShrink method, sub-optimal universal threshold and identical neighboring window size in all wavelet sub-bands are used. However, in the proposed method, instead of sub-optimal universal threshold, an optimal threshold is determined for every wavelet sub-band by the Stein's Unbiased Risk Estimate (SURE). Denoising is performed on images represented in rectangular grid as well as hexagonal grid using modified thresholding method for comparison. MSE, PSNR and SSIM are used for the performance analysis. The obtained results confirm that the proposed method gives better results than existing algorithms.

Keywords: Wavelet thresholding, Denoising, Hexagonal lattice, Gabor filter, Interpolation

1. INTRODUCTION

Digital image processing is mainly used for improving or enhancing the pictorial information for human interpretation and processing image data for storage transmission and representation. At present all the images have square shaped pixels and hence all the image processing algorithms are done on the same basis. Processing based on hexagonal grid is a new approach in the field of image processing, because of its various advantages.

Hexagonal image processing is a new developing area of image processing, in which the images are represented by using hexagonal shaped pixels rather than square pixels. Image processing in hexagonal grid is very much advantageous than in the conventional rectangular grid. The advantages include higher angular resolution, consistent connectivity, higher sampling efficiency, etc.

* Corresponding author.
E-mail address: jeevanjeevan77@gmail.com (Jeevan K. M.).

Peer Review under the responsibility of Universidad Nacional Autónoma de México.

Usually digital images are mapped on square lattice. In hexagonal image processing we change the square lattice to hexagonal lattice by re-sampling the images.

Image denoising is one of the major challenges in the field of image processing and computer vision. Image denoising is the process of estimating the original image by suppressing noise from a noisy image. Usually the noise is introduced in the images during image acquisition (digitization) or during image transmission. Sensor temperature and light levels are major factors that affect the amount of noise in the images while acquiring images with CCD camera. Also, images are corrupted during transmission. A noisy image can be mathematically expressed as shown in Eq. (1).

$$I_N(x,y) = I(x,y) + N(x,y) \tag{1}$$

where *I(x,y)* is the original image, *N(x,y)* is the noise, and $I_N(x,y)$ is the resulting noisy image. Typical noises usually present in an image are uniform or quantization noise, salt & pepper noise, Gaussian noise, Gamma noise, Rayleigh distribution noise, etc. (Jaiswal, Upadhyay, & Somkuwar, 2004). In this work we focus on Gaussian noise present in an image.

In Gaussian noise the noise having a probability density function (PDF) equal to that of the normal distribution, which is also known as the Gaussian distribution (i.e., the values that the noise can take on are Gaussian-distributed). The probability density function 'p' of a Gaussian random variable 'z' is given by

$$p(z) = \frac{1}{\sigma\sqrt{2\pi}} e^{-\frac{(z-\mu)^2}{2\sigma^2}} \tag{2}$$

where μ is the mean value and σ is the standard deviation. In the case of images z represents the grey level. A special case is white Gaussian noise, in which the values at any pair of times are identically distributed and statistically independent. A lot of algorithms have been proposed to improve the performance of image denoising scheme. All these works are based on the images on rectangular grid. Wavelet thresholding based image denoising by representing images in hexagonal grid using the modified NeighShrink thresholding is mentioned in this work.

The paper is organized as follows. Section 2 is devoted for literature review which includes brief introduction to discrete wavelet transform, wavelet thresholding, and concepts of hexagonal image processing and related works.

In Section 3 we introduce the proposed methodology of image denoising using JeevKrish (Jeev: first four letters of the name of the first author, Krish: first five letters of the name of the second author) thresholding in hexagonal domain. Results and discussion, and conclusions are given in sections 4 and 5, respectively.

2. LITERATURE REVIEW

2.1 DISCRETE WAVELET TRANSFORM (DWT)

A wavelet is a waveform of an effectively limited duration that has an average value of zero. A function ψ(x) can be called a wavelet if it possesses the following properties:

1.- The function integrate to zero, or equivalently, its Fourier transform denoted as ψ(ω) is zero at the origin.

$$\int_{-\alpha}^{\alpha} \psi(x)dx = 0 \tag{3}$$

2.- It is square integrable, or equivalently, has finite energy

$$\int_{-\alpha}^{\alpha} |\psi(x)|^2 dx < \alpha \tag{4}$$

Eq. (3) suggests that the function is either oscillatory or has a wavy appearance and Eq. (4) implies that most of the energy in ψ(x) is confined to a finite interval or in other words ψ(x) has good space localization.

The discrete wavelet transform (DWT) is obtained by filtering the signal through a series of digital filters at different scales. The scaling operation is done by changing the resolution of the signal by the process of subsampling. In the computation of DWT, the input image is decomposed into low-pass and high-pass sub-bands, i.e., each decomposition stage consists of a low-pass filter (LPF) and a high-pass filter (HPF). When the signal passes through these filters, it splits into two bands. The LPF, which corresponds to an averaging operation, extracts the coarse information of the signal. The HPF, which corresponds to a differencing operation, extracts the detailed information of the signal. The output of the filtering operation is then decimated by two. In the case of images (two-dimensional signal), first, the image is filtered along the row and decimated by two.

Then it is followed by filtering the sub-image along the column and decimated by two. This operation splits the image into four bands namely LL (Low frequency or approximation coefficient), LH (vertical details), HL (horizontal details), and HH (diagonal details) as shown in Figure 1.

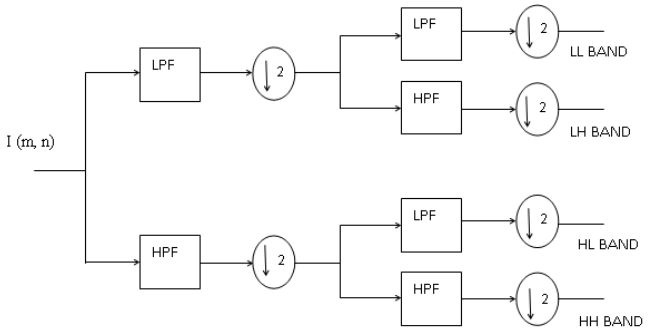

Fig. 1. First Level Wavelet Decomposition.

2.2 WAVELET THRESHOLDING

Denoising by thresholding in wavelet domain was developed by Donoho and Johnstone (1995). In wavelet domain, large coefficients correspond to the signal and small ones represent mostly the noise. The thresholding of wavelet coefficients is done by either 'Hard' or 'Soft' thresholding function.

In hard thresholding (Figure 2(a)) the wavelet coefficients below the threshold 'T' are made zero and coefficients above the threshold are not changed. If 'x' and 'y' represent the input and output respectively, then the hard thresholding is given by the equation

$$x = T_h(y,T) = \begin{cases} y, if\ |y| \geq T \\ 0, otherwise \end{cases} \quad (5)$$

In the case of soft thresholding (Fig. 2(b)), the wavelet coefficients are shrunk towards zero by a threshold value 'T'. It can be represented by the equation

$$x = T_s(y,T) = \begin{cases} y - T, if\ y \geq T \\ y + T, if\ y \leq -T \\ 0, \ otherwise \end{cases} \quad (6)$$

Selection of low value of threshold may produce a result which is near to the input, but the result still may be noisy. Larger value of threshold produces an output with large number of zero coefficients. The result of this selection is a very smooth signal. The smoothness suppresses the details and edges of the original image and causing blurring and ringing artifacts. Some of the existing methods in the literature for estimating the threshold are described below.

VisuShrink

This technique consists of applying the soft thresholding operator using the universal threshold proposed by Donoho and Johnstone (1995) and this threshold is given by the equation

$$T_{visu} = \sigma_n \sqrt{2logL} \quad (7)$$

where σ_n^2 is the noise variance of Adaptive White Gaussian Noise (AWGN) and 'L' represents the total number of pixels in the image. This method gives a highly smoothed reconstruction of the noisy image, but we have to compromise many of the important features of the image as the threshold tends to be high for large values of 'L' and this may eliminate the signal coefficient along with noise.

SureShrink

Thresholding method that minimizes the Stein Unbiased Risk Estimator (SURE) developed by Donoho and Johnstone (1995) is known as SureShrink wavelet thresholding technique. This method select distinct threshold for each sub-band of each level of the wavelet tree and hence it is known as an adaptive method for selecting threshold. The SureShrink threshold T_{sure} is expressed as

$$T_{sure} = \min\left(t, \sigma\sqrt{2logL}\right) \quad (8)$$

where 't' represents the value that minimize the Stein Unbiased Risk Estimator (SURE), σ^2 is the noise variance and L is the size of the image.

BayesShrink

The threshold derived in a Bayesian approach is given by the equation

$$T_B = \left(\frac{\sigma_n^2}{\sigma_F}\right) \quad (9)$$

where σ_n^2 is the estimated noise variance of AWGN by robust median estimator and $\sigma_F$is the estimated signal standard deviation in wavelet-domain. The robust median estimator is given by the equation

$$\sigma_n = \frac{Median[\![\{Y_{ij}\}]\!]}{0.6745}, Y_{ij} \in Subband \quad (10)$$

NeighShrink

Chen, Bui, and Krzyzak (2004) proposed a new wavelet thresholding method in their paper titled 'Image denoising using neighbouring wavelet coefficients' called NeighShrink. It is the modification of wavelet denoising scheme for 1D signal by incorporating neighboring coefficients in the thresholding process proposed by Cai & Silverman (2001). In NeighShrink method, the wavelet coefficients are thresholded according to the value of the squared sum of all the values of wavelet coefficients in the neighborhood window. The window size can be taken as 3X3, 5X5, 7X7, etc. In Chen et al. (2004) it is already reported that 3X3 window gives better results. The shrinkage for NeighShrink is expressed as

$$\beta_{ij} = \left(1 - \frac{T_u^2}{S_{ij}^2}\right) \quad (11)$$

where S_{ij}^2 is the squared sum of all wavelet coefficients in the selected window and T_u is the universal threshold. If S_{ij}^2 is less than or equal to T_u^2 , then the wavelet coefficient (C_{ij}) to be modified is set to zero. Otherwise it is modified according to

$$C_{ij} = C_{ij}\beta_{ij} \quad (12)$$

Some other thresholding methods are SmoothShrink method proposed by Mastriani and Giraldez (2007) for images corrupted by speckle noise. Another method called BiShrink, based on non-Gaussian bivariate distributions model proposed by Sendur & Selesnick (2002a, 2002b). Shengqian, Yuanhua, and Daowen (2002) proposed an adaptive shrinkage denoising scheme using neighborhood characteristics and they claimed that their scheme produced better results than the results produced by Donoho (1995) and Donoho et al. (1995).

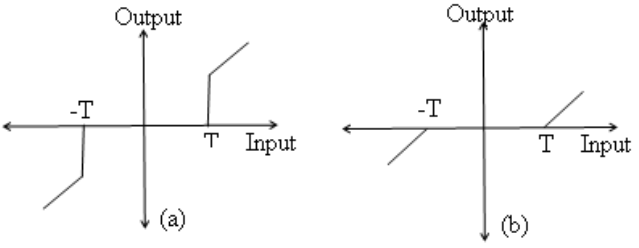

Fig. 2. (a) Hard Thresholding, (b) Soft Thresholding First.

2.3 HEXAGONAL IMAGE PROCESSING

The photoreceptors (Rods & Cones) of human retina closely resemble to hexagonal structure (Curcio, Sloan, Kalina, & Hendrickson, 1990). Figure 3 shows the arrangement of rods & cones in human retina. Since the cells in human retina have hexagonal structure, the image developed in the retina has hexagonal shaped pixels. In addition, hexagonal geometry has some advantages like higher sampling efficiency, consistent connectivity and higher angular resolution. Due to these reasons many researchers have studied the possibility of representing digital images with hexagonal pixels (Barun, Pooja & Kuldip, 2014; Middleton & Sivaswamy, 2005; Veni & Narayanankutty, 2011). But the non-availability of hardware for capturing and displaying hexagonal based images limits the use of hexagonal image structure for further processing. Since there is no hardware for capturing the hexagonal images, conversion has to be done from square to hexagonal image before hexagonal-based image processing.

There have been several ways to simulate a hexagonal grid on a regular rectangular grid. The common simulations methods are re-sampling the square lattice to the hexagonal lattice, mimic hexagonal pixels using square pixels, pseudo hexagonal pixel, and virtual hexagonal structure.

One method of representing hexagonal lattice using the simulation method - resampling the square lattice to the hexagonal lattice - is alternate pixel suppressal method (Sankar, Sanjay & Rajan, 2004). Hexagonal grid image based on alternate pixel suppressal method can be obtained from the conventional image by alternatively suppressing rows and columns of the existing rectangular grid and sub-sampling it. All the other pixels of the rectangular grid which do not have any correspondence with the hexagonal counterparts are suppressed to zero.

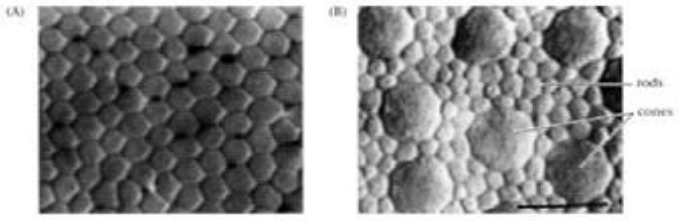

Fig. 3. Arrangement of rods and cones in human retina.

While processing this sub-sampled image the suppressed pixels are not considered in computation. The sub-sampled hexagonal grid is shown in Figure 4.

Image processing applications like image rotation, edge detection, etc. in hexagonal lattice have already been discussed by many researchers. Middleton and Jayanthi Sivaswamy (2001) proposed an edge detection method in a hexagonal image processing framework. In this work the authors conclude that the hexagonal framework gives better results for edge detection. Veni, and Narayanankutty (2011), Vidya et al. (2009) and Vidya (2011) also analyzed the performance of edge detection on hexagonal sampling grid. Comparisons of image alignment on hexagonal and square lattices were performed by Shima, Sugimoto, & Okutomi (2010). Azam, Anjum, & Javed (2010) proposed discrete cosine transform based method for face recognition in hexagonal images. Wavelet based image compression in hexagonal domain was proposed by Jeevan & Krishnakumar (2014) in the paper titled 'Compression of images represented in hexagonal lattice using wavelet and Gabor filter'. In all these works, the authors confirmed that the hexagonal representation gives better results.

In this paper we propose an image denoising method in hexagonal lattice using wavelet thresholding method. Modified NeighShrink method, which is explained in the next section, is used for thresholding.

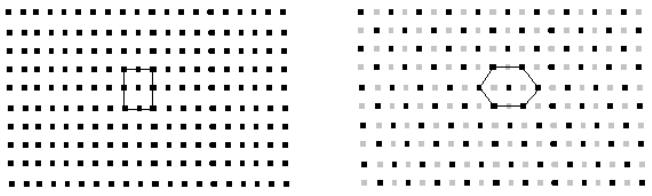

Fig. 4. (a) Rectangular grid and (b) Simulated hexagonal grid obtained using alternate pixel suppression.

3. PROPOSED METHODOLOGY

An image denoising method using modified NeighShrink thresholding method named as JeevKrish thresholding is proposed in our work. Although the work proposed is image denoising, we are trying to confirm that the hexagonal representation is better than the normal square pixel representation of images. We consider images corrupted with Gaussian noise. Figure 5 shows the block diagram of the proposed method.

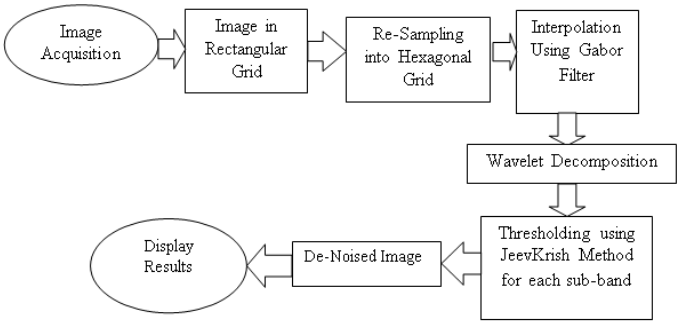

Fig. 5. Block Diagram for the Proposed Method.

Due to the non-availability of hardware for acquiring hexagonal images, rectangular grid to hexagonal grid conversion has to be done before performing hexagonal image processing. In this work we use alternate pixel suppressal method, which is explained in Section 2.3 for simulating the hexagonal grid from rectangular grid. During the conversion of images from rectangular lattice to the hexagonal lattice, considerable loss in image quality was observed. So, image reconstruction through interpolation is used. Interpolation using Gabor filter is used in this work.

Gabor filter (Gabor, 1946; Vidya, 2011) is the only filter with orientation selectivity that can be expressed as a sum of two separable filters. In the spatial domain, a 2D Gabor filter is a Gaussian kernel function modulated by a sinusoidal plane wave. The following equations represent the 2D-Gabor function which was proposed by Daugman (1985). Equations 13 and 14 represent the real and imaginary part of the function, respectively.

$$g_{\lambda\theta\sigma_{\gamma\varphi}}(x,y) = \exp\left(-\frac{x'^2 + \gamma^2 y'^2}{2\sigma^2}\right)\cos\left(2\pi\frac{x'}{\lambda} + \varphi\right) \quad (13)$$

$$g_{\lambda\theta\sigma_{\gamma\varphi}}(x,y) = \exp\left(-\frac{x'^2 + \gamma^2 y'^2}{2\sigma^2}\right)\sin\left(2\pi\frac{x'}{\lambda} + \varphi\right) \quad (14)$$

where $x' = x\cos\theta + y\sin\theta$ and $xy' = -x\sin\theta + y\cos\theta$

The arguments 'x' and 'y' specify the position of 'x' and 'y' coordinate of the image and sigma (σ), gamma (γ), lambda (λ), theta (∈), and phi (ϕ) are parameters as follows. The standard deviation (σ) of the Gaussian factor determines the size of the receptive field. The parameter gamma (γ) named as aspect ratio, specifies the ellipticity of the Gaussian factor. It has been found to vary in a limited range of $0.23 < \gamma < 0.92$. The parameter lambda (λ) is the wavelength and 1/λ the spatial frequency of the cosine factor in Eq. (13). The ratio σ/λ determines the spatial frequency bandwidth.

The interpolation is done using Gabor filter in the following manner. Hexagonal sampled grid has directional symmetry in 0^0, 60^0, and 120^0 orientations. Due to these three axes of symmetry of hexagonal grid, we select three different orientation of Gabor filter along in 0^0, 60^0, and 120^0, and the filtering is done in these three orientations (Jeevan et al., 2014). The three filtered images in these three orientations are then superimposed to get the interpolated image.

The filtered image is then decomposed using wavelet to get four sub-bands namely LL, LH, HL and HH. LL is the low frequency sub-band and most of the image details are present in this sub-band. LH, HL, and HH contain high frequency components and hence most of the noises are present in these bands. Therefore, thresholding is done on all the coefficients in LH, HL, and HH sub-bands. This thresholding is done using JeevKrish method which is explained below.

Let C_{ij} be the wavelet coefficients in the sub-band.

Select the neighborhood window as shown in Figure 6 with size 3X3 and C_{ij} as the center element.

1. Calculate

$$S_{i,j}^2 = C_{i-1,j-1}^2 + C_{i-1,j}^2 + C_{i-1,j+1}^2 + C_{i,j-1}^2 + C_{i,j}^2 + C_{i.j+1}^2 + C_{i+1,j-1}^2 + C_{i+1,j}^2 + C_{i+1,j+1}^2 .$$

if

{

$S_{i,j}^2$ is less than or equal to T_{sure}^2, the wavelet coefficient $C_{i,j}$ is set to zero.

}

else

{

$$C_{ij} = C_{ij}\left(1 - \frac{T_{Sure}^2}{S_{ij}^2}\right)$$

}

Where T_{Sure} is the threshold obtained using SureShrink.

As explained in Section 2.2 SureShrink is the thresholding method that minimizes the Stein Unbiased Risk Estimator (SURE). This method selects distinct threshold for each sub-band of each level of the wavelet tree and get an optimal threshold value compared to the universal thresholding. The SureShrink threshold T_{sure} is expressed as

$$T_{sure} = \min\left(t, \sigma\sqrt{2logL}\right)$$

where 't' represents the value that minimize the Stein Unbiased Risk Estimator (SURE), σ^2 is the noise variance and L is the size of the image. So the thresholding factor for JeevKrish thresholding can be expressed as

$$\partial_{i,j} = \left(1 - \frac{T_{sure}^2}{S_{ij}^2}\right) \quad (15)$$

Therefore, the shrinkage rule is; if $S_{i,j}^2$ is less than or equal to T_{sure}^2, the coefficient $C_{i,j}$ is set to zero. Otherwise $C_{i,j} = C_{i,j}\partial_{i,j}$, where, $\partial_{i,j}$ is the proposed shrinkage factor. Using this shrinkage rule, thresholding is done on each wavelet coefficient by selecting 3X3 neighborhood window. Soft thresholding is performed in this process. Finally perform inverse wavelet transform on the thresholded wavelet coefficient to get the denoised image.

The proposed denoising algorithm can be summarized as follows:

1. Convert the noisy image in rectangular grid to hexagonal grid using alternate pixel suppressal method.
2. Perform Gabor filter interpolation on hexagonal grid image.
3. Perform wavelet decomposition on the image obtained after step 2.
4. Threshold the wavelet coefficients in the sub-bands LH, HL, and HH using the proposed JeevKrish method choosing 3X3 neighborhood window size.
5. Perform inverse wavelet transform on the thresholded wavelet coefficient to get the denoised image.

This method gives better results compared to other shrinkage methods like VisuShrink, SureShrink, and NeighShrink and also it is better than the MATLAB denoising function 'wdencmp'.

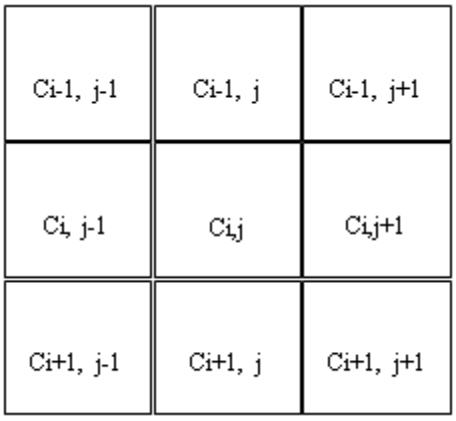

Fig. 6. 3X3 Neighborhood Window with Ci,j, the coefficient to be thresholded, at the center.

4. RESULTS AND DISCUSSION

The proposed JeevKrish denoising method is performed on more than hundred images. This paper gives importance for performing denoising using proposed method in hexagonal domain. The hexagonal grid is obtained using alternate pixel suppressal method and interpolation using Gabor filter. The Gabor filtering is done in three different orientations along in 0^0, 60^0, and 120^0. This filtering helps to remove noises in high frequency region. The test results for all these images in terms of Mean Square Error (MSE) and Peak Signal to Noise Ratio (PSNR) indicate that the denoising performance is better in hexagonal domain. In addition to MSE and PSNR, we also used structural similarity (SSIM) for analyzing the performance. SSIM also indicate that the performance is better in hexagonal domain. The performances of proposed method on conventional images are better than the denoising using NeighShrink, VisuShrink and SureShrink_methods. It also performed better than the MATAB de-noising function 'wdencmp' and if we represent the images in hexagonal lattice, the performance of the proposed method again improves and gives better Mean Square Error (MSE) and Peak Signal to Noise Ratio (PSNR). These results confirm that the hexagonal representation is better than the conventional rectangular lattice.

In NeighShrink, $S_{i,j}^2$ obtained is compared with T_u^2, where T_u is the universal threshold which does not deals with minimizing MSE and hence eliminate many coefficients. But in the case of JeevKrish thresholding, the proposed method $S_{i,j}^2$ is compared with T_{sure}^2, the SureShrink threshold. It is based on Stein's Unbiased Risk Estimator (SURE) and it minimizes mean squared error and gives an optimal threshold value which is better than T_u. In JeevKrish method, each coefficient in each sub-band is thresholded using this optimal threshold value. We are also considering the effect of neighbor coefficients for thresholding the coefficient $C_{i,j}$. So this method gives better results than other methods.

MSE and PSNR, two commonly used measures for quantifying the error between images, are used for the performance analysis. MSE indicate the average difference of the pixel throughout the image. If MSE is higher the difference of the pixel between the original and the processed image is also higher. The MSE between two images P and Q is defined by

$$MSE = \frac{1}{N}\sum_i \sum_j (Q_{ij} - P_{ij})^2 \tag{16}$$

where the sum over 'i' and 'j' denotes the sum over all pixels in the images, and 'N' is the total number of pixels in each image. The PSNR between two images is given by

$$PSNR = 10log_{10}\left(\frac{255^2}{MSE}\right) \tag{17}$$

SSIM is another parameter used for the performance analysis. It is used for measuring similarity between two images. "The MSE or PSNR estimate absolute errors on the other hand, SSIM is a perception-based model that considers image degradation as perceived change in structural information, while also incorporating important perceptual phenomena, including both luminance masking and contrast masking terms (Wang Zhou et al, 2004).

The obtained PSNR for five different images are represented in Table 1. Graphical representation of 'MSE vs. σ' for the image 'elephant.jpg' is shown in Figure 7. Experiments are performed on more than hundred images. Figure 8(a – f) and Figure 9(a – f) shows the test result for two different images 'car.jpg' with $\sigma = 30$ and 'lena.png' with $\sigma = 40$. Table 2 gives a comparison of SSIM for conventional square grid images and hexagonal grid images.

A statistical analysis is also done for the performance comparison. Analysis of Variance (ANOVA) is used for the analysis of the methods presented in this paper. Data sets used for the statistical analysis and the details of

analysis are presented in Table 3, 4 and 5 respectively. From the table it is clear that the 'F' value is greater than 'F-Critical' which indicate there is significant difference between the methods and also it is seen that the average value of PSNR is greater for the proposed method. So we can conclude that our method gives better results.

Table 1.
MSE &PSNR obtained for five different images for different σ.

Noise Level (σ)	**Test Images**	**MATLAB Function (wdencmp)**		**JeevKrish (Proposed Method)**			
		Rectangular Grid Image		Rectangular Grid Image		**Hexagonal Grid Image**	
		MSE	PSNR	MSE	PSNR	MSE	PSNR
10	car.jpg	17.576	35.6816	14.7061	36.4558	**2.6659**	**43.8723**
	elephant.jpg	30.2087	33.3295	18.1072	35.5523	**9.6699**	**38.2766**
	flower.jpg	20.141	35.09	17.6277	35.6688	**2.2797**	**44.5521**
	barbara.png	40.9523	32.008	25.7547	34.0222	**13.0611**	**36.971**
	lena.png	23.5426	34.4123	19.979	35.1251	**3.7642**	**42.3741**
20	car.jpg	43.2053	31.7754	42.5185	31.845	**3.155**	**43.1409**
	elephant.jpg	45.6756	31.534	42.1588	31.8819	**11.7425**	**37.4332**
	flower.jpg	44.7033	31.6274	44.4646	31.6507	**3.1774**	**43.1101**
	barbara.png	57.7775	30.5132	52.8348	30.9016	**14.3789**	**36.5536**
	Lena.png	46.6498	31.4423	46.612	31.4458	**4.6889**	**41.4201**
30	car.jpg	63.6594	30.0922	63.6157	30.0952	**4.0735**	**42.0311**
	elephant.jpg	57.7272	30.517	55.9205	30.6551	**13.9895**	**36.6728**
	flower.jpg	65.0948	29.9943	64.7502	30.0184	**5.2854**	**40.9**
	barbara.png	73.0098	29.497	70.8848	29.6253	**15.7914**	**36.1466**
	lena.png	66.3655	29.9114	66.0229	29.9339	**5.8342**	**40.471**
40	car.jpg	77.052	29.263	76.9681	29.2677	**5.9666**	**40.3735**
	elephant.jpg	67.7233	28.8234	65.0718	29.9969	**17.9162**	**35.5983**
	flower.jpg	78.336	29.1912	78.0755	29.2057	**9.3387**	**38.4279**
	barbara.png	82.6824	28.9567	81.5699	29.0155	**18.023**	**35.5725**
	lena.png	79.1361	29.1471	78.3899	29.1882	**7.487**	**39.3877**
50	car.jpg	85.8141	28.7952	85.8648	28.7927	**6.1066**	**40.2728**
	elephant.jpg	73.2895	29.4804	72.1936	29.5458	**22.0585**	**34.695**
	flower.jpg	86.9257	28.7393	87.3004	28.7206	**15.3704**	**35.9323**
	barbara.png	90.0086	28.588	90.0932	28.5839	**22.3416**	**34.6397**
	lena.png	86.9196	28.7396	87.0679	28.7322	**10.2045**	**38.0429**

Table 2.
SSIM obtained for Square Grid and Hexagonal Grid Images.

Test Images Noise Level (σ) is 20	**SSIM**	
	Rectangular Grid Image	Hexagonal Grid Image
Image1	0.4869	**0.6856**
Image2	0.4771	**0.585**
Image3	0.5403	**0.6496**
Image4	0.5537	**0.5818**
Image5	0.5102	**0.643**
Image6	0.5228	**0.557**
Image7	0.3889	**0.6931**
Image8	0.3855	**0.673**
Image9	0.4935	**0.5865**
Image10	0.393	**0.6008**

Table 3.
Data Sets Used for ANOVA.

	Denoising Using JeevKrish (proposed) Method in Hexagonal Grid Image	**Denoising Using JeevKrish (proposed) Method in Rectangular Grid Image**	**Denoising Using MATLAB Function (wdencmp)**
PSNR for 5 different test images (Noise Level σ = 10)	43.8723	36.4558	35.6816
	38.2766	35.5523	33.3295
	44.5521	35.6688	35.09
	36.971	34.0222	32.008
	42.3741	**35.1251**	**34.4123**

Table 4.
Analysis of Variance (ANOVA) – Summary.

Groups	**Count**	**Sum**	**Average**	**Variance**
Denoising Using JeevKrish (proposed) Method in Hexagonal Grid Image	5	206.0461	41.20922	11.54664
Denoising Using JeevKrish (proposed) Method in Rectangular Grid Image	5	176.8242	35.36484	0.794471
Denoising Using MATLAB Function (wdencmp)	5	170.5214	34.10428	2.137283

Table 5.
Analysis of Variance (ANOVA) – Table of ANOVA.

Source of Variation	SS	df	MS	F	P-value	F crit
Between Groups	143.7099	2	71.85497	14.88873	0.000562	3.885294
Within Groups	57.91357	12	4.826131			
Total	201.6235	14	To			

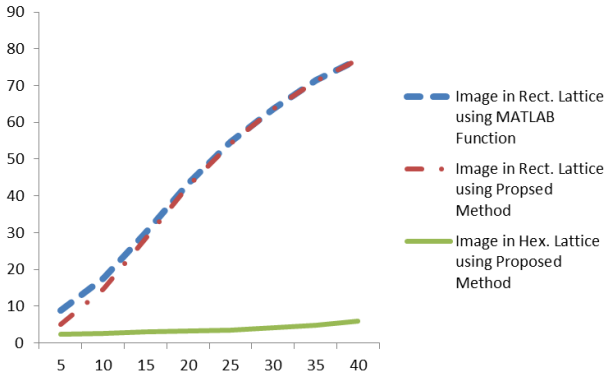

Fig. 7. MSE vs. σ for the image 'elephant.jpg'.

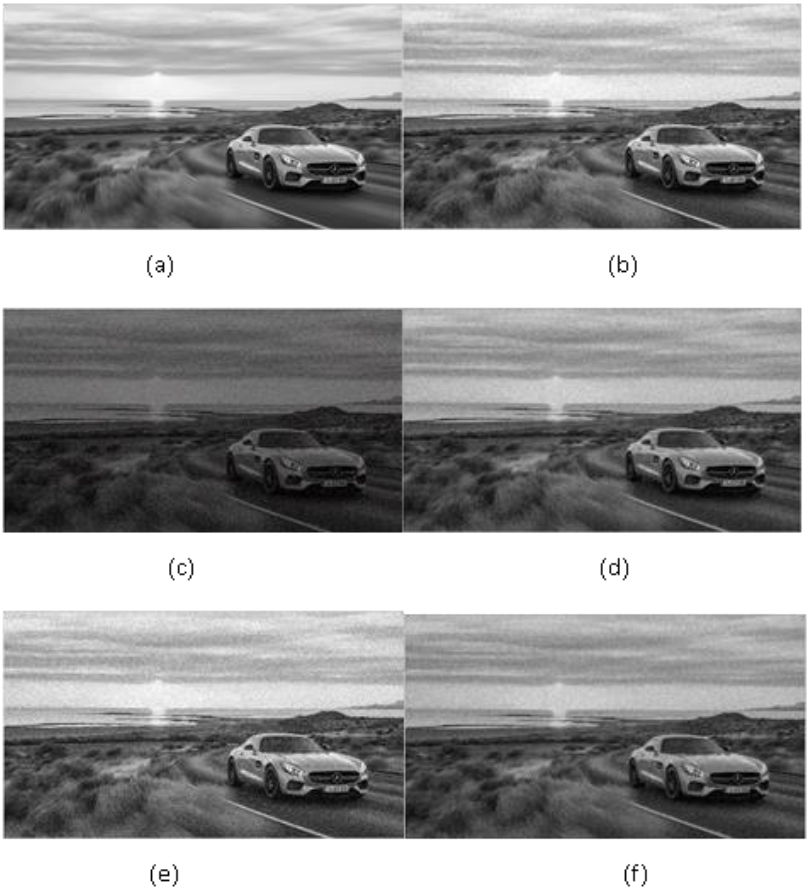

Fig. 8. (a) Original image (b) Noisy Image σ =30, (c) Noisy image in Hexagonal lattice (d) Image after interpolation using Gabor filter (e) De-noised image in Rectangular lattice (f) De-noised image in Hexagonal Lattice.

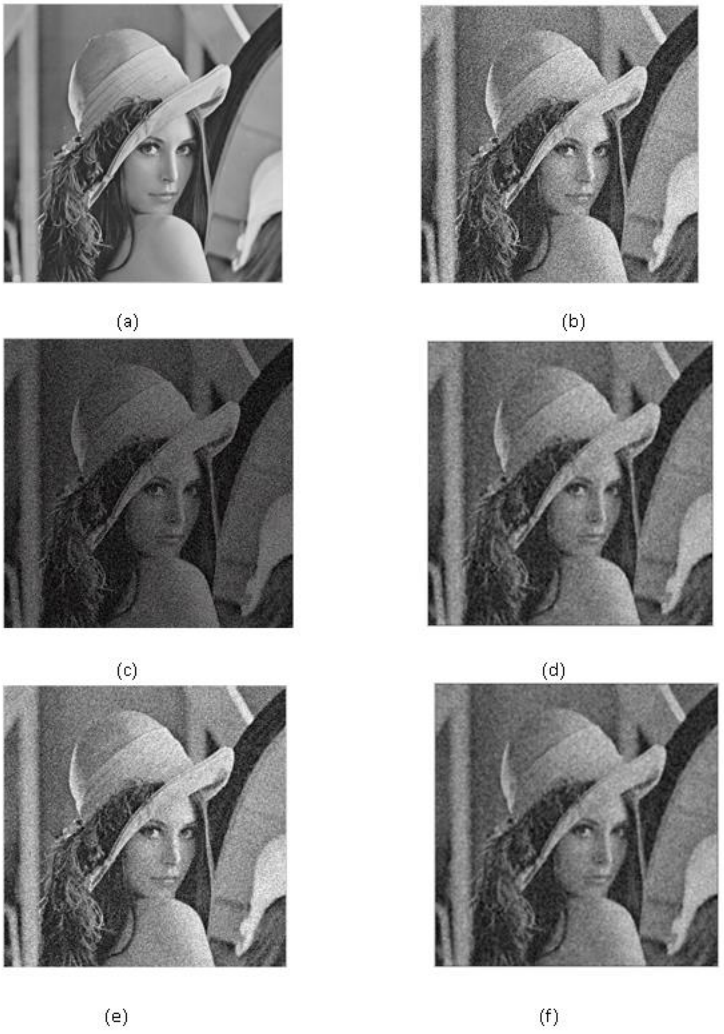

Fig. 9. (a) Original image (b) Noisy Image σ =40, (c) Noisy image in Hexagonal lattice (d) Image after interpolation using Gabor filter (e) De-noised image in Rectangular lattice (f) De-noised image in Hexagonal Lattice.

5. CONCLUSION

We simulated the proposed method and it has been found that the images represented in hexagonal domain gives better results than conventional images. Also the proposed method is better than the denoising function 'wdencmp' used in MATLAB. MSE, PSNR and SSIM are found to be better in hexagonal domain. Combining wavelet and processing of images in hexagonal grid, we achieved a better result than conventional methods, because hexagonal wavelet includes the advantage of hexagonal grid along with the wavelet. Also it gives the missing corner stone of artificial human visual system.

CONFLICT OF INTEREST

The authors have no conflicts of interest to declare.

REFERENCES

Azam, M., Anjun, M. A., & Javed, M. Y. (2010). Discrete cosine transform (DCT) based face recognition in hexagonal images. *The 2nd IEEE International Conference on Computer and Automation Engineering,* (Vol. 2, pp. 474-479). IEEE.

Barun, K., Pooja, G., & Kuldip, P. (2014). Square pixels to hexagonal pixel structure representation technique. *International Journal of Signal Processing*, Image Processing and Pattern Recognition, 17(4), 137-144 doi:10.14257/ijsip.2014.7.4.13

Cai, T. T., & Silverman, B. W. (2001). *Incorporating information on neighbouring coefficients into wavelet estimation*. Sankhya: The Indian Journal of Statistics, 63, 127-148.

Chen, G. Y., Bui, T. D., & Krzyzak, A. (2004). *Image denoising using neighbouring wavelet coefficients*, IEEE International Conference on Acoustics, Speech, and Signal Processing, II917-II920.

Curcio, C. A., Sloan, K. R., Kalina, R. E., & Hendrickson, A. E. (1990). Human photoreceptor topography. *Journal of comparative neurology*, *292*(4), 497-523.

Daugman, J. G. (1985). Uncertainty relation for resolution in space, spatial frequency, and orientation optimized by two-dimensional visual cortical filters. *JOSA A*, *2*(7), 1160-1169.

Donoho, D. L. (1995). De-noising by soft-thresholding. *IEEE transactions on information theory*, 41(3), 613-627.

Donoho, D. L., & Johnstone, I. M. (1995). Adapting to unknown smoothness via wavelet shrinkage. *Journal of the american statistical association*, *90*(432), 1200-1224.

Gabor, D. (1946). Theory of communication. Part 1: The analysis of information. *Journal of the Institution of Electrical Engineers-Part III: Radio and Communication Engineering*, *93*(26), 429-441.

Jaiswal, A., Upadhyay, J., & Somkuwar, A. (2004). Image denoising and quality measurements by using filtering and wavelet based techniques. *International Journal of Electronics and Communications (AEÜ)*, 68(8), 699–705, doi:10.1016/j.aeue.2014.02.003.

Jeevan, K. M., & Krishnakumar, S. (2014). Compression of images represented in hexagonal lattice using wavelet and Gabor filter. *Proceedings of 2014 IEEE International Conference on Contemporary Computing and Informatics*, pp 609–613.

Mastriani, M. & Giraldez, A. E. (2007). Smoothing of coefficients in wavelet domain for speckle reduction in synthetic aperture radar images, *Journal of Graphics Vision and Image Processing*, 7, 1-8.

Middleton, L., & Sivaswamy, J. (2005), Hexagonal image processing – A practical approach, USA, Springer-Verlag London Limited.

Middleton, L., & Sivaswamy, J. (2001). Edge detection in a hexagonal-image processing framework. *Image and Vision computing*, *19*(14), 1071-1081.

Sankar, K. P., Sanjay, T., & Rajan, E. G. (2004). Hexagonal Pixel Grid Modelling and Processing of Digital Images using CLAP Algorithms. *International Conference on Systemic*, Cybernetics and Informatics.

Sendur, L., & Selesnick, I. W. (2002a). Bivariate shrinkage functions for wavelet-based denoising exploiting inter-scale dependency. *IEEE Trans. Signal Processing*, 50(11), 2744–2756.

Sendur, L., & Selesnick, I. W. (2002b). Bivariate shrinkage with local variance estimation. *IEEE Signal Process.* Lett. 9(12), 438–441.

Shengqian, W., Yuanhua, Z. & Daowen, Z. (2002*)*. Adaptive shrinkage denoising using neighbourhood characteristic. *Electronics Letters*, 38(11), 502-503.

Shima,T., Sugimoto, S., & Okutomi, M. (2010). Comparison of image alignment on hexagonal and square lattice. *Proceedings of 2010 IEEE 17th International Conference on Image Processing*, pp 141–144.

Veni, S., & Narayanankutty, K. A. (2011). Gabor functions for interpolation on hexagonal lattice. *International Journal of Electronics & Communication Technology*, 2(1), 15-19.

Vidya, P. (2011). Gabor Wavelet Based Edge detection on Hexagonal sampled Grid. *International Journal of Electronics & Communication Technology*, 2(2), 122–125.

Vidya, P., Veni, S., & Narayanankutty, K. A. (2009). Performance analysis of edge detection methods on hexagonal sampling grid. *International Journal of Electronic Engineering Research*, 1(4), 313–328.

Wang Zhou, Bovik, Alan C., Sheikh, Hamid R., and Simoncelli Eero P. (2004). Image Quality Assessment: From Error Visibility to Structural Similarity. *IEEE Transactions on Image Processing*, Volume 13, Issue 4, pp. 600–612